EUROPHYSICS LETTERS 1 November 2002

*Europhys. Lett.*, **60** (3), pp. 467–473 (2002)

# Multiscale modeling of anisotropic wet chemical etching of crystalline silicon

M. A. Gosálvez, A. S. Foster and R. M. Nieminen

*Laboratory of Physics, Helsinki University of Technology*
*P.O. Box 1100, 02015 Espoo, Finland*

(received 30 April 2002; accepted 15 August 2002)

PACS. 81.65.Cf – Surface cleaning, etching, patterning.
PACS. 71.15.-m – Methods of electronic structure calculations.

**Abstract.** – We combine *ab initio* and Monte Carlo simulations in multiscale modelling of anisotropic wet chemical etching of silicon. The anisotropy of the macroscopic etching patterns observed in the experiments is explained by two mechanisms at an atomistic scale: the weakening of backbonds following OH termination of surface sites and the existence of significant interaction between the surface-terminating species (H and OH). For the first time, we demonstrate that the H/OH and OH/OH interactions have an essential role, directly controlling the appearance of the fastest-etched planes in the macroscopic etching patterns.

Anisotropic wet chemical etching of silicon in alkaline solutions [1] is one of the key techniques for the manufacture of microsystems. However, the mechanisms responsible for the strong crystalline anisotropy of the etch rates are not completely understood. It is generally thought that hydroxyl ions $OH^-$ present in the etching solution play a central role, catalyzing the removal of surface silicon atoms by weakening the backbonds after substituting the surface-terminating hydrogen atoms [2]. In this letter, we show how subtle features of the microscopic reaction environment lead to dramatic changes in the macroscopic etching patterns. In particular, we show for the first time that the geometrical restrictions imposed by the presence of a specific type of next-nearest neighbours are crucial for the appearance of such important features of the macroscopic etching patterns as the fastest-etched planes. This is done by combining atomistic total-energy calculations with large-scale Monte Carlo simulations for the etching kinetics.

A number of techniques for the simulation of anisotropic wet chemical etching have been presented in the literature [3]. Of all possible approaches, only *atomistic models* enable the identification of the essential microscopic mechanisms which control the complicated electrochemical reactions [2] between the surface atoms and the molecules and ions of the etching solution. In these models, the probability of removal of a surface atom is "controlled" by its neighbourhood, since it determines the number and type of backbonds which need to be broken. The number of bonds is determined by the number of first neighbours, and their energy (*i.e.* the bond *type*), by the number of OH groups terminating both the surface atom and the first neighbours, as shown in fig. 1. This dependence of the removal of a surface atom on the

© EDP Sciences

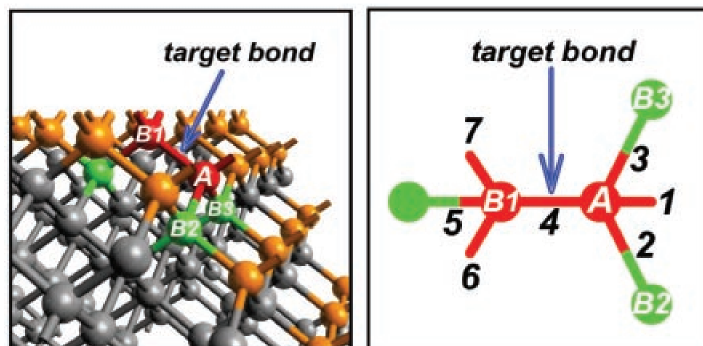


Fig. 1 – Real structure (left) and schematic representation (right) of one of the 8 possible bond types. The OH termination of surface atoms is represented by dangling bonds. The 8 possible configurations are obtained as the number of dangling bonds (*i.e.* OH groups) is varied from 0 to 3 on each atom sharing the target bond and only different configurations are counted [4]. The configuration shown, denoted as 2-1 ("2 dangling bonds on the left and 1 on the right"), is identical to 1-2. The configurations 0-0 and 3-3 do not have any physical meaning since the former describes a bond between two bulk atoms and the latter a free molecule not linked to the rest of the system. Note that the removal of target atom A requires breaking bonds 2, 3 and 4 to the first neighbours B1-B3. Since OH-termination of the surface atoms results in the weakening of the backbonds, the energy required to break, *e.g.*, target bond 4 depends not only on the number of OH groups attached to atom A (the target atom) but also on the number of OH groups attached to atom B1 (a first neighbour). Similar reasonings will apply to backbonds 2 and 3 when each is in turn considered as the target bond.

number of OH groups terminating its first neighbours (backbond weakening) can be understood as a dependence on the number of next-nearest neighbours, because the hydroxyl groups are located at the positions occupied earlier by next-nearest neighbours of the surface atom [3]. There is, however, one more way in which the next-nearest neighbours can affect the removal of a surface atom and which has not been taken into account in any previous study before. A detailed consideration of the neighbourhood of a surface atom shows that there exist two types of second neighbours, here referred to as "direct" and "indirect" (fig. 2). A *direct second neighbour* (such as any of C1 through C6) is linked to the target atom A *directly* through a first neighbour (either B1 or B2). However, an *indirect second neighbour* (such as C7/C8) is not linked to the target atom through a first neighbour, because this one is missing. In this case an *indirect* (longer) path along the bonding structure has to be followed in order to reach the target atom A starting from C7/C8. As the figure shows, the indirect neighbours are important in order to distinguish between certain environments (otherwise the two environments shown for target atom A would actually be identical). Intuitively, one would expect that the presence of the indirect second neighbours would impose additional geometrical restrictions on the hydroxyl termination of the target atom. In this letter we demonstrate that the macroscopic features of the etching process are strongly sensitive to these geometrical restrictions.

The surface of silicon can be either H-terminated or OH-terminated during the etching process depending on the concentration of the etchant and the *p*H value [5]. However, even in the case of H dominance, OH groups will still terminate a significant fraction of the surface sites [2], providing the mechanism for further etching. Besides, the slow reaction step for the formation of a Si complex solvable in the solution is the first substitution of a terminating H by an OH, after which the sequence of further chemical steps is fast [2]. Additional experimental evidence [6] implies the existence of OH clustering at the initially OH-terminated sites in an

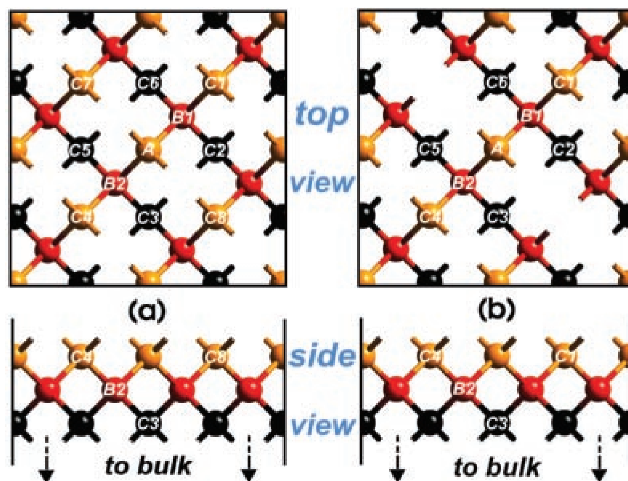


Fig. 2 – (a) The target atom A represents a typical atom of an ideal (100) surface. It has 2 first neighbours (B1-B2) and 8 second neighbours (C1-C8). C1 through C6 are *direct* second neighbours, because they are linked to the target atom A *directly* through a first neighbour (B1 for C1, C2 and C6; B2 for C3, C4 and C5). However, C7 and C8 cannot be linked to A by the corresponding first neighbours, because they are missing. (b) The neighbourhood of atom A has now only 6 second neighbours (C2-C7). Note that in this case C7 and C8 do not restrict the attachment of hydroxyl groups OH on A as they do in (a).

otherwise "fully" H-terminated surface. As a result, hydroxyl termination of the target atom and its first neighbours is present even in the case of hydrogen termination. For the rest of the surface atoms (including the second neighbours of the target atom), one type of termination or the other will exist depending on the *p*H and the OH-coverage conditions. In this work, only the average effect of coverage is considered. The effects of specific OH-coverages are discussed in detail in [7].

We have carried out electronic-structure calculations in order to clarify how bond weakening occurs and how the indirect second neighbours affect the removal of surface atoms. The *ab initio* calculations were performed with the Amsterdam Density Functional (ADF) code [8], implementing the density functional theory (DFT) using the gradient-corrected BLYP functional [9,10]. The code uses Slater-type basis functions and all atoms calculated are represented by triple-zeta basis sets with two polarization functions, with frozen inner orbitals. Atoms are relaxed to minimize total energy and atomic forces using a conjugate gradient algorithm.

To model the hydrogen/hydroxyl–covered silicon surface we consider an H-terminated $Si_{18}$ cluster with adsorbed hydroxyl groups at various different sites, as shown in fig. 3. This cluster is produced by taking a section out of the (100) silicon surface, freezing the bottom two layers at the experimental geometry and then fully relaxing the remaining atoms. Calculated vibrational frequencies for Si-H, O-H and Si-O bonds in this cluster show excellent agreement [7] with experimental surface values [11,12], demonstrating the suitability of the cluster model for representing surface processes. In order to calculate the bond-breaking energies for different surface environments, we used 10 different cluster configurations, where each cluster has from 0 to 2 hydroxyl groups adsorbed on the top three Si atoms. After calculating the relaxed total energy for the cluster configuration, the apex atom (and any H and/or OH bonded to it) is separated (as a neutral unit) from the rest of the cluster. The relaxed total energy was

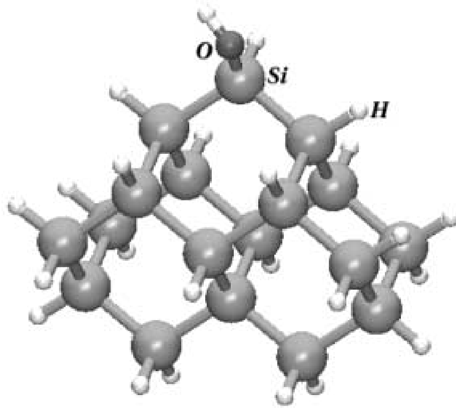


Fig. 3 – $Si_{18}$ H-terminated cluster used to simulate the silicon surface in *ab initio* calculations. This cluster has a single hydroxyl group adsorbed on the apex and represents an example of the ten different hydroxyl configurations studied.

then recalculated with the separated Si frozen. The difference between the normal and separated total energy for one configuration provides the bond-breaking energy for a specific set of bonds, and by combining the results from all ten configurations a complete atom removal energy hierarchy is produced.

The calculations show that each bond is weakened by an amount $\epsilon$ ($\approx 0.4\,\text{eV}$) for every OH group that is attached to either atom sharing the bond. In this way, there is no dependence on whether the hydroxyl groups are adsorbed at the apex or side atoms, only the total number of them determines the removal energy. Using the notation of fig. 1, the energy of an $i$-$j$ bond ($i, j = 0, 1, 2, 3$) can be therefore written as

$$\epsilon_{ij} = \epsilon_0 - (i + j) \cdot \epsilon,$$

where $\epsilon_0$ is the bond energy between two bulk atoms ($\epsilon_0 \approx 2.7\,\text{eV}$). This means, *e.g.*, that breaking a 2-1 bond costs the same energy as breaking a 3-0 bond.

To investigate the role of indirect second neighbours, we expand the configuration seen in fig. 3, so that it includes two identical indirect second neighbours and a total of 44 silicon atoms. In this way, the initial smaller cluster models the situation pictured on the right-hand side of fig. 2 and the current expanded cluster models the left-hand side. Similarly as with the smaller cluster, we calculate the total energy of the relaxed cluster and a cluster with the middle apex Si atom removed. In this case we are breaking effectively the same bonds, but the surrounding environment has changed. As a result, each one of the two broken bonds is about 0.2 eV easier to break than in the smaller cluster, the main contribution coming from the relaxation energy of neighbouring H and OH groups on the indirect sites. We thus conclude that *it costs more energy to add an* OH *group to a silicon site with indirect neighbours.*

The *ab initio* analysis points out that the effect of the indirect second neighbours is *geometrical* in origin: the termination probability of a dangling bond by a hydroxyl group decreases if indirect second neighbours are present, due to the extra interaction between the hydroxyl group and the hydrogen terminating the indirect neighbour. This extra interaction, however, has no significant effects when the chosen atom has only one first neighbour, because the atom can rotate about the direction of the bond and minimize in this way the interaction between the hydroxyl (attached to the chosen atom) and the hydrogen (attached to the indirect sec-

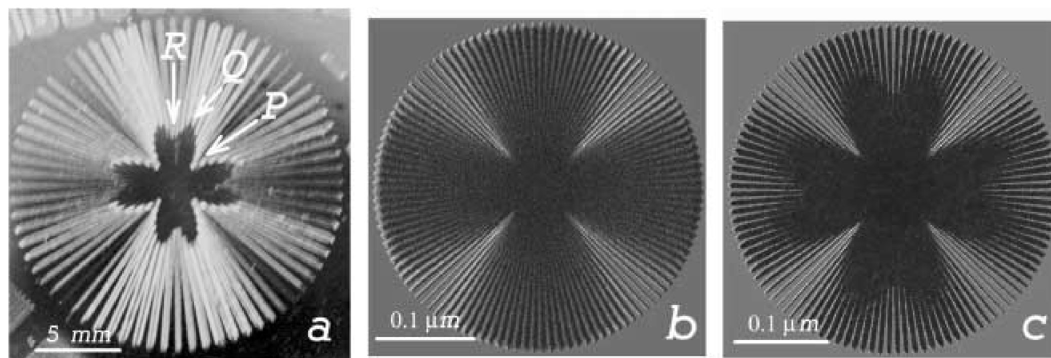


Fig. 4 – Comparison between (a) experiment [3], (b) simulation using the "bond-weakening" approach and (c) simulation incorporating the effect of indirect second neighbours.

ond neighbour). However, if the chosen atom has two or three first neighbours, the rigidity of the bond configuration leads to a significant interaction between the hydroxyl group and the terminating hydrogen, effectively reducing the probability with which the hydroxyl will actually terminate the dangling bond in the presence of an indirect second neighbour. These considerations imply that the probability of removal of a surface atom should be multiplied by the probability with which each hydroxyl group will actually terminate the corresponding dangling bond depending on the local environment.

We have discussed here the interaction between a hydroxyl terminating the target atom and a hydrogen terminating an indirect second neighbour. Similarly, we can consider the interaction with another hydroxyl. The effect of having both interactions can only be discussed in a frame that considers the amount of surface coverage by hydroxyl groups [7]. However, the conclusions of the present study are not affected by considering an *average* of the effect of both interactions.

In order to use the above results in kinetic Monte Carlo simulations, we consider the probability of removal of a surface atom as given by the Boltzmann expression $p = \mathrm{e}^{-\Delta E/k_\mathrm{B}T}$, where $\Delta E$ is defined as the energy excess of the average energy per bond $\overline{E}$ (defined below) over a critical energy $E_\mathrm{c}$:

$$\Delta E = k_\mathrm{B}T \ln\left[1 + \mathrm{e}^{(\overline{E}-E_\mathrm{c})/k_\mathrm{B}T}\right] \approx \max(0, \overline{E} - E_\mathrm{c}).$$

The critical energy $E_\mathrm{c}$ acts as a threshold below which bond-breaking occurs with probability $p \approx 1$. The average energy per bond $\overline{E}$ is assigned to the chosen surface atom depending on the neighbourhood configuration, and is defined in terms of the energy matrix $\epsilon_{ij}$ discussed previously. We identify each surface atom with its neighbourhood configuration, referred to by $(n; m_1, m_2, \ldots, m_n; l)$, meaning that the chosen surface atom has $n$ first neighbours $(n = 1, 2, 3)$ and each of the $n$ first neighbours has itself $m_j$ first neighbours $(j = 1, 2, \ldots, n;$ $m_j = 1, 2, 3, 4)$, $l$ of which are indirect second neighbours to the chosen atom. The average energy per bond $\overline{E}$ for atom $(n; m_1, m_2, \ldots, m_n; l)$ is then defined as

$$\overline{E} = \frac{1}{n}\sum_{j=1}^{n} \epsilon_{(4-n),(4-m_j)} + l \cdot e \cdot (1 - \delta_{1n}).$$

The first term corresponds simply to the average of the sum of the energies of the bonds to the $n$ first neighbours, the energy of each bond being obtained by looking at the number of

hydroxyls attached to both atoms sharing the bond ($i = 4 - n$ and $j = 4 - m_j$). The second term incorporates the effect from indirect neighbours. It contains an additional average energy $e$ for each indirect second neighbour present ($e \approx 0.2\,\mathrm{eV}$ according to the DFT calculations) so that, effectively, the probability of removal is multiplied by the probability of OH termination in the presence of indirect neighbours. $\delta_{ij}$ is the "Kronecker delta" ($\delta_{ij} = 1$ if $i = j$ and $\delta_{ij} = 0$ if $i \neq j$), used in order to add the extra term only in the case that the number of first neighbours $n$ is 2 or 3, as described previously.

The previous expression for the removal probability $p$ is incorporated into a continuous Monte Carlo scheme [13] developed from a discrete Monte Carlo scheme [3]. In order to validate the model, we consider the etching of Si(100) wafers masked by a typical wagon-wheel pattern [14]. It should be noticed that the use of such a mask causes the apparition of all possible microscopic configurations for a surface atom at any of the $(hkl)$ surfaces enforced by the $\langle hk0 \rangle$-aligned masking spokes. This mask is thus a difficult test for any model aimed at explaining the etching process. In fig. 4 we first compare experiment (a) and a Monte Carlo simulation (b) using $\epsilon_0 = 2.7\,\mathrm{eV}$, $\epsilon = 0.4\,\mathrm{eV}$, $E_\mathrm{c} = 2.1\,\mathrm{eV}$, $T = 348\,\mathrm{K}$ and $e = 0\,\mathrm{eV}$. We note that $\epsilon_0$ and $\epsilon$ are taken from the DFT calculations and $T$ is set by the experiment ($75\,^\circ\mathrm{C}$). By making $e = 0\,\mathrm{eV}$, we can evaluate the effect from bond weakening only (no indirect second-neighbour effects). The value of $E_\mathrm{c}$ is fitted to give best agreement with experiment. The simulation describes well the features of the anisotropic pattern at the regions around the $\langle 110 \rangle$ wafer directions (region P) but the full anisotropy of the experimental pattern is not obtained. In particular, the features at regions Q and R are not predicted. This means that the (111) planes are well differentiated from the rest of the cystallographic planes, but the fastest-etched planes are not predicted correctly. In frame (c) we present a Monte Carlo simulation that incorporates the effect from the indirect second neighbours. This is done by setting $e = 0.13\,\mathrm{eV}$ while keeping the other parameters as above. We note that $e$ is fitted to the experiment, guided by the *ab initio* estimate (0.2 eV). By direct comparison with frames (a) and (b) we conclude that the correct prediction of the fastest-etched planes (region Q) is clearly controlled by the incorporation of the indirect second neighbours in the simulation. It is remarkable that such an important macroscopic feature of the etching process is actually due to the geometrical restrictions imposed by the indirect second neighbours on the termination probability of dangling bonds by hydroxyl groups.

In conclusion, the anisotropy of wet chemical etching at the macroscopic scale is explained by two mechanisms at the atomistic scale: the weakening of backbonds following OH termination of surface atoms and the existence of significant interaction between the terminating H atoms and OH groups. In particular, we have demonstrated for the first time that the H/OH and OH/OH interactions control the appearance of the fastest-etched planes and, therefore, the macroscopic features of the etched patterns.

* * *

This research has been supported by the Academy of Finland. We thank P. Sushko and A. Ayuela for useful discussions.

REFERENCES

[1] Lang W., *Mater. Sci. Eng. R: Rep. Rev. J.*, **17** (1996) 1.
[2] Allongue P., *Phys. Rev. Lett.*, **77** (1996) 1986.
[3] Gosálvez M. A., Nieminen R. M., Kilpinen P., Haimi E. and Lindroos V., *Appl. Surf. Sci.*, **178** (2001) 7.

[4] Camon H., Moktadir Z. and Djafari-Rouhani M., *Mater. Sci. Eng. B*, **37** (1996) 142.
[5] Cerofolini G. F. and Meda L., *Appl. Surf. Sci.*, **89** (1995) 351.
[6] Pietsch A. J., Higashi G. S. and Chabal Y. J., *Appl. Phys. Lett.*, **64** (1994) 3115.
[7] Gosálvez M. A., Foster A. S. and Nieminen R. M., to be published in *Appl. Surf. Sci.* (2002).
[8] Te Velde G. *et al.*, *J. Comp. Chem.*, **22** (2001) 931.
[9] Becke A. D., *Phys. Rev. A*, **38** (1988) 3098.
[10] Lee C., Yang W. and Parr R. G., *Phys. Rev. B*, **37** (1988) 785.
[11] Weldon M. K., Stefanov B. B., Raghavachari K. and Chabal Y. J., *Phys. Rev. Lett.*, **79** (1997) 2851.
[12] Ibach H., Wagner H. and Bruchmann D., *Solid State Commun.*, **42** (1982) 457.
[13] Zhu Z. and Liu C., *Comput. Mod. Eng. Sci.*, **1** (2000) 11.
[14] Seidel H., Csepregi L., Huberger A. and Baumgartel H., *J. Electrochem. Soc.*, **137** (1990) 3612.